Portal Venous 5-Aminoimidazole-4-Carboxamide-1-β-D-Ribofuranoside Infusion Overcomes Hyperinsulinemic Suppression of Endogenous Glucose Output

Raul C. Camacho, R. Richard Pencek, D. Brooks Lacy, Freyja D. James, E. Patrick Donahue, and David H. Wasserman

AMP-activated protein kinase (AMPK) plays a key role in regulating metabolism, serving as a metabolic master switch. The aim of this study was to assess whether increased concentrations of the AMP analog, 5-aminoimidazole-4-carboxamide-1-β-D-ribosyl-5-monophosphate, in the liver would create a metabolic response consistent with an increase in whole-body metabolic need. Dogs had sampling (artery, portal vein, hepatic vein) and infusion (vena cava, portal vein) catheters and flow probes (hepatic artery, portal vein) implanted >16 days before a study. Protocols consisted of equilibration (−130 to −30 min), basal (−30 to 0 min), and hyperinsulinemic-euglycemic or -hypoglycemic clamp periods (0–150 min). At $t = 0$ min, somatostatin was infused and glucagon was replaced in the portal vein at basal rates. An intraportal hyperinsulinemic (2 mU · kg^{-1} · min^{-1}) infusion was also initiated at this time. Glucose was clamped at hypoglycemic or euglycemic levels in the presence (H-AIC, $n = 6$; E-AIC, $n = 6$) or absence (H-SAL, $n = 6$; E-SAL, $n = 6$) of a portal venous 5-aminoimidazole-4-carboxamide-ribofuranoside (AICAR) infusion (1 mg · kg^{-1} · min^{-1}) initiated at $t = 60$ min. In the presence of intraportal saline, glucose was infused into the vena cava to match glucose levels seen with intraportal AICAR. Glucagon remained fixed at basal levels, whereas insulin rose similarly in all groups. Glucose fell to 50 ± 2 mg/dl by $t = 60$ min in hypoglycemic groups and remained at 105 ± 3 mg/dl in euglycemic groups. Endogenous glucose production (R_a) was similarly suppressed among groups in the presence of euglycemia or hypoglycemia before $t = 60$ min and remained suppressed in the H-SAL and E-SAL groups. However, intraportal AICAR infusion stimulated R_a to increase by 2.5 ± 1.0 and 3.4 ± 0.4 mg · kg^{-1} · min^{-1} in the E-AIC and H-AIC groups, respectively. Arteriovenous measurement of net hepatic glucose output showed similar results. AICAR stimulated hepatic glycogen to decrease by 5 ± 3 and 19 ± 5 mg/g tissue ($P < 0.05$) in the presence of euglycemia and hypoglycemia, respectively. AICAR significantly increased net hepatic lactate output in the presence of hypoglycemia. Thus, intraportal AICAR infusion caused marked stimulation of both hepatic glucose output and net hepatic glycogenolysis, even in the presence of high levels of physiological insulin. This stimulation of glucose output by AICAR was equally marked in the presence of both euglycemia and hypoglycemia. However, hypoglycemia amplified the net hepatic glycogenolytic response to AICAR by approximately fourfold. *Diabetes* 54:373–382, 2005

From the Department of Molecular Physiology and Biophysics, Diabetes Research and Training Center, Vanderbilt University School of Medicine, Nashville, Tennessee.

Address correspondence and reprint requests to Dr. Raul Camacho, Department of Molecular Physiology and Biophysics, Vanderbilt University School of Medicine, Nashville, TN 37232-0615. E-mail: raul.camacho@vanderbilt.edu.

Received for publication 15 July 2004 and accepted in revised form 2 November 2004.

ACC, acetyl-CoA carboxylase; AICAR, 5-aminoimidazole-4-carboxamide-ribofuranoside; AMPK, AMP-activated protein kinase; HPLC, high-performance liquid chromatography; NHGO, net hepatic glucose output; SRIF, somatostatin; ZMP, 5-aminoimidazole-4-carboxamide-1-β-D-ribosyl-5-monophosphate.

Iatrogenic hypoglycemia is the number one short-term complication for type 1 (1) and type 2 (2) diabetic patients striving to maintain tight glycemic control. This results from inappropriate relative hyperinsulinemia. Physical activity sensitizes the body to hyperinsulinemia, thereby increasing this risk of hypoglycemia (3). Current treatments for hypoglycemia include carbohydrate ingestion or, if necessary (i.e., during unconsciousness), administration of exogenous glucagon. However, depending on the level of hyperinsulinemia, neither of these treatments may be sufficient. A more optimal treatment would be one that is effective in the presence of hyperinsulinemia.

AMP-activated protein kinase (AMPK) plays a key role in regulating carbohydrate and fat metabolism, serving as a metabolic master switch in response to alterations in cellular energy charge (4). Liver (5,6) and muscle (7–9) AMPK is activated and its downstream target, acetyl-CoA carboxylase (ACC), is phosphorylated (inactivated) during exercise. AMPK can be pharmacologically stimulated by 5-aminoimidazole-4-carboxamide-ribofuranoside (AICAR), which enters cells and is rapidly phosphorylated to 5-aminoimidazole-4-carboxamide-1-β-D-ribosyl-5-monophospate (ZMP) (10), an AMP analog. Administration of AICAR causes marked breakdown of muscle (11) and liver (12) glycogen, which is a hallmark response to sustained exercise as well as pathways that are inhibited by hyperinsulinemia. Although this process has been attributed to ZMP-stimulation of AMPK (11) and the resultant activation of phosphorylase kinase (13), myocardial glycogen degradation has also been shown to be due to allosteric activation of glycogen phosphorylase by an AICAR-induced elevation of ZMP (14). Another recent study found that AICAR activated glycogenolysis primarily by stimulating

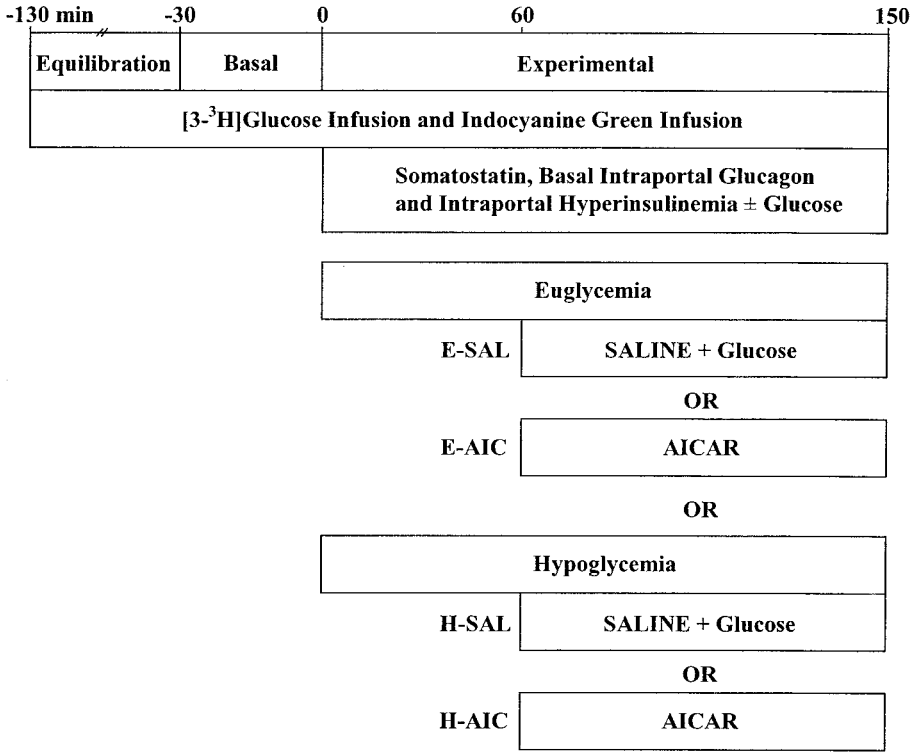

FIG. 1. Experimental protocol. All protocols consisted of a dye and isotope equilibration period (−130 to −30 min), a basal sampling period (−30 to 0 min), and a hyperinsulinemic-euglycemic or hypoglycemic clamp (somatostatin plus basal intraportal glucagon) period (0−150 min) in which saline or AICAR (1 mg · kg^{-1} · min^{-1}) was infused intraportally from 60 to 150 min. See RESEARCH DESIGN AND METHODS for infusion rates of isotope and hormones.

glycogen phosphorylase allosterically and not through the AMPK signaling pathway (15). AICAR activates glycogen phosphorylase and counteracts the inhibitory effect of glucose-6-phosphate on this enzyme (16).

Despite compelling evidence for an important role of AMPK in muscle, little is known about its glucoregulatory role in other tissues that are also important in sustaining energy metabolism. Our laboratory has recently shown in the conscious dog that intraportal AICAR abolishes net hepatic glucose uptake and can even stimulate net hepatic glucose output (NHGO) when infused at 1 and 2 mg · kg^{-1} · min^{-1}, respectively, to rates as high as those achieved during exercise (17) when the liver was in a glycogen storage mode (high insulin, high glucose, and negative arterial-portal venous glucose difference). These responses are consistent with the concept that increased AMP concentrations not only signal increased glucose metabolism within the muscle, but also coordinate a whole-body response that increases the availability of blood glucose by preventing its uptake by the liver, where it is normally stored as glycogen. Therefore, we wanted to test the hypothesis that increasing the concentrations of the AMP analog, ZMP, in the liver would create a metabolic response consistent with an increase in whole-body metabolic need during the metabolic stress of insulin-induced hypoglycemia. To this end, we infused AICAR intraportally (at rates 10% of those used in rodent models to minimize extrahepatic effects) (18–20) during euglycemic and hypoglycemic glucose clamps in which somatostatin (SRIF) was infused, glucagon was replaced at basal rates, and insulin was replaced at high physiological levels.

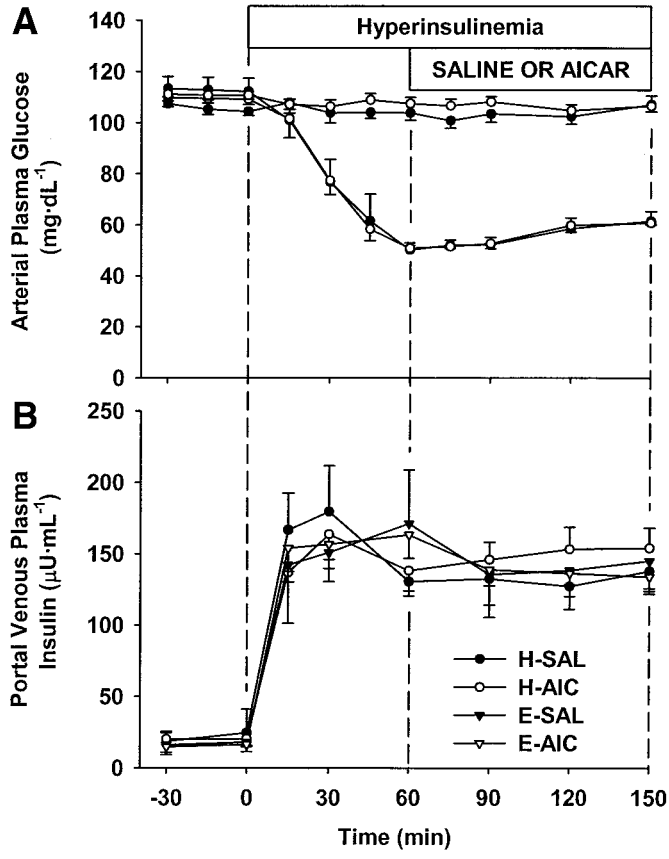

FIG. 2. Arterial plasma glucose (*A*) and portal venous plasma insulin (*B*) in the H-SAL (●), H-AIC (○), E-SAL (▲), and E-AIC (△) groups during the basal period (−30 to 0 min) and hyperinsulinemic-euglycemic or -hypoglycemic clamp period (0−150 min) in the presence or absence of intraportal AICAR from 60 to 150 min. Data are means ± SE.

RESEARCH DESIGN AND METHODS

Experiments were performed on 23 overnight-fasted mongrel dogs (mean wt 23.2 ± 0.4 kg) of either sex that had been fed a standard diet (Pedigree beef

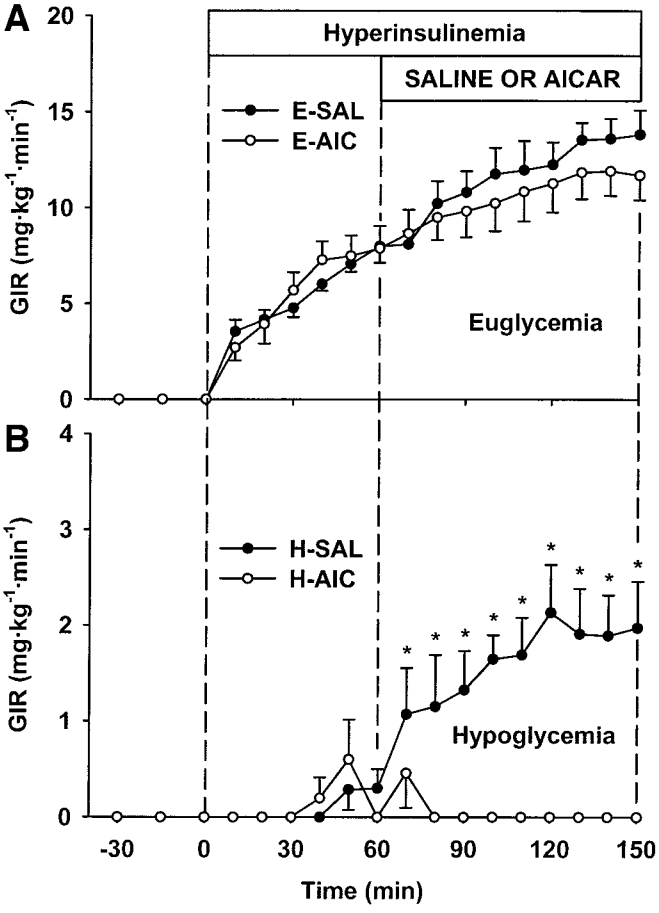

FIG. 3. Glucose infusion rate in the saline (●) and AICAR (○) groups during the basal period (−30 to 0 min) and hyperinsulinemic-euglycemic (*A*) or -hypoglycemic (*B*) clamp period (0−150 min) in the presence or absence of intraportal AICAR from 60 to 150 min. Data are means ± SE. *Significantly different than the H-AIC group ($P < 0.05$).

dinner and Wayne Lab Blox; 51% carbohydrate, 31% protein, 11% fat, and 7% fiber based on dry wt) and given free access to water. Animals were housed under controlled temperature (21°C) and lighting conditions, with 12 h of light (6 A.M. to 6 P.M.) and 12 h of dark (6 P.M. to 6 A.M.). Protocols were approved by the Vanderbilt University Animal Care Committee.

At least 16 days before each experiment, a laparotomy was performed under general anesthesia (0.04 mg/kg of atropine and 15 mg/kg pentobarbital sodium before surgery and 1.0% isofluorane inhalation anesthetic during surgery). Catheters were inserted in portal and hepatic veins for blood sampling. An incision was made over the femoral artery into which a silastic catheter (inside diameter 0.04 in) was inserted and advanced to the level of the distal aorta (~16 cm) for sampling and hemodynamic measurements during experiments. Silastic catheters (inside diameter 0.03 in) were inserted into the vena cava for infusions. A silastic catheter (inside diameter 0.03 in) was inserted into the splenic vein and positioned so that the catheter tip rested just beyond the point where the splenic and portal veins coalesce. This catheter was used for the intraportal infusions of glucagon, insulin, and AICAR. Catheters were filled with heparinized saline, and the free ends were knotted. Ultrasonic transit time flow probes were fitted and secured to the portal vein and hepatic artery (Transonic Systems, Ithaca, NY). The knotted catheter ends and flow probe leads were stored in a subcutaneous pocket in the abdominal region, so that the complete closure of skin incisions was possible.

Blood samples were drawn 3 days before the experiment to determine the leukocyte count and hematocrit of the animal. Only animals with *1*) a leukocyte count <18,000/mm^3, *2*) a hematocrit >36%, *3*) a good appetite (consumption of daily food ration), and *4*) normal stools were used.

All studies were conducted in dogs fasted for 18 h. Free catheter ends and flow probe leads were accessed through small skin incisions made under local anesthesia in the abdominal and leg regions the morning of the experiment. The contents of the catheters were then aspirated and flushed with saline.

Experiments consisted of a tracer equilibration period (−130 to −30 min), a basal period (−30 to 0 min), and a hyperinsulinemic-hypoglycemic or -euglycemic clamp period (0−150 min). A primed (40 μCi) infusion (0.2 μCi/min) of [3-^{3}H]glucose purified by high-performance liquid chromatography (HPLC) was initiated at $t = -130$ min. The tracer infusion rate was tripled at $t = 0$ min in euglycemic groups. A constant-rate indocyanine green infusion (0.1 mg · m^{-2} · min^{-1}) was also started at $t = -130$ min and continued throughout the study. Indocyanine green was used as a backup method of blood flow measurement (21) if the Doppler probes did not provide a clear signal and as confirmation of hepatic vein catheter placement. A peripheral infusion of SRIF (0.8 μg · kg^{-1} · min^{-1}) was started at $t = 0$ min to inhibit endogenous insulin and glucagon secretion. Concurrent with the infusion of SRIF was basal intraportal glucagon replacement (0.5 ng · kg^{-1} · min^{-1}). An intraportal hyperinsulinemic infusion (2 mU · kg^{-1} · min^{-1}) was also initiated at this time. Arterial glucose was clamped at euglycemic levels (~105 mg/dl) or allowed to fall to hypoglycemic levels (~50 mg/dl). In one hyperinsulinemic-hypoglycemic (H-AIC, $n = 6$) and hyperinsulinemic-euglycemic (E-AIC, $n = 6$) protocol, a portal venous infusion of AICAR (1 mg · kg^{-1} · min^{-1}) was initiated at $t = 60$ min (Fig. 1). In a second hyperinsulinemic-hypoglycemic (H-SAL, $n = 6$) and hyperinsulinemic-euglycemic (E-SAL, $n = 5$) protocol, a portal venous infusion of saline was initiated at $t = 60$ min. Two initial H-AIC studies were performed to determine target glycemic responses for glucose clamping. All other experiments were randomized. In the H-SAL group, glucose was infused into the vena cava to match the increase in glucose seen in the H-AIC protocol. Portal vein and hepatic artery blood flows were monitored on-line throughout the experiments. At the end of the experiment, animals were killed with sodium pentobarbital and an autopsy was performed to confirm catheter placement. Liver biopsies were frozen in liquid nitrogen for later analyses. Blood samples were taken to determine circulating liver enzymes (alanine aminotransferase, aspartate aminotransferase, γ-glutamyl transpeptidase, and lactate dehydrogenase).

Blood sample and tissue collection and processing. Arterial, portal vein, and hepatic vein blood samples were drawn at $t = -30, -15, 0, 15, 30, 45, 60, 75, 90, 120$, and 150 min in all groups. Arterial blood samples were taken every 10 min to determine plasma glucose−specific activity. Plasma glucose concentrations and radioactivity were determined as previously described (22). Blood samples were deproteinized (1 ml blood in 3 ml of 4% perchloric acid), and whole blood alanine, β-hydroxybutyrate, glycerol, and lactate concentrations were determined using standard enzymatic methods (23). Free fatty acids, cortisol, catecholamines, and immunoreactive insulin and glucagon were measured as previously described (22). Hepatic concentrations of glycogen were measured using enzymatic methods (after digestion of precipitated glycogen with amyloglucosidase) by the method of Chan and Exton (24). Hepatic purine nucleotide concentrations were determined from liver samples homogenized in 0.4 mol/l perchloric acid with 0.5 mmol/l EGTA and neutralized with 0.5 mol/l potassium carbonate (pH 6.8). HPLC analysis and ultraviolet detection were performed to assess nucleotide levels in the samples as previously described (25,26).

Western blotting. Liver samples (~50 mg) were homogenized in a solution containing 10% glycerol, 20 mmol/l Na-pyrophosphate, 150 mmol/l NaCl, 50 mmol/l HEPES (pH 7.5), 1% NP-40, 20 mmol/l β-glycerophosphate, 10 mmol/l NaF, 2 mmol/l EDTA (pH 8.0), 2 mmol/l phenylmethylsulfonyl fluoride, 1 mmol/l $CaCl_2$, 1 mmol/l $MgCl_2$, 10 μg/ml aprotinin, 10 μg/ml leupeptin, 2 mmol/l Na_2VO_3, and 3 mmol/l benzamide. Homogenized samples were assayed for protein concentration using a Pierce BCA protein assay kit (Rockford, IL). Next, 30 μg of protein were run on a SDS-PAGE gel and transferred to a polyvinylidine fluoride membrane. Membranes were treated with rabbit α-phospho-AMPK (Thr^{172}) or α-phospho-acetyl-CoA carboxylase (Ser^{79}) (Cell Signaling, Beverly, MA) and then incubated with anti-rabbit horseradish peroxidase (Promega, Madison, WI). Chemiluminescence was detected with a WesternBreeze kit (Invitrogen, Carlsbad, CA). Densitometry was performed using Scion Image software (Frederick, MD).

Calculations. Net hepatic uptake of alanine, β-hydroxybutyrate, free fatty acids, glycerol, and lactate and NHGO were determined as [HAF × (H − A)] + [PVF × (H − P)], in which A, P, and H are the arterial, portal vein, and hepatic vein concentrations, and HAF and PVF are the hepatic artery and portal vein blood flows. The difference in glycogen due to AICAR was calculated as Gly(H-SAL) − Gly(H-AIC) and Gly(E-SAL) − Gly(E-AIC), where Gly(H-SAL) and Gly(E-SAL) are the average hepatic glycogen levels in the respective groups, and Gly(H-AIC) and Gly(E-AIC) are the individual hepatic glycogen levels in AICAR-treated dogs in the presence of hypoglycemia and euglycemia, respectively. Endogenous glucose production (R_a) and glucose utilization (R_d) were determined by isotope dilution (27).

Statistical analysis. Statistical comparisons among groups and over time were made using ANOVA designed to account for repeated measures. Specific time points were examined for significance using contrasts solved by univariate repeated measures. Liver purine nucleotides were compared using ANOVA. Liver glycogen was compared using t tests. AMPK and ACC phos-

TABLE 1
Arterial plasma insulin, glucagon, cortisol, epinephrine, and norepinephrine levels during baseline and hyperinsulinemic-euglycemic and -hypoglycemic clamp periods in the presence or absence of intraportal AICAR

		Hyperinsulinemia					
					±Intraportal AICAR		
	Basal	15 min	30 min	60 min	90 min	120 min	150 min
Arterial plasma insulin (μU/ml)							
E-SAL	6 ± 1	41 ± 4	41 ± 4	45 ± 5	45 ± 5	44 ± 5	45 ± 5
E-AIC	6 ± 0	38 ± 6	44 ± 9	45 ± 8	48 ± 9	53 ± 7	55 ± 7
H-SAL	8 ± 2	36 ± 5	37 ± 5	39 ± 6	42 ± 7	44 ± 7	42 ± 5
H-AIC	8 ± 1	36 ± 2	36 ± 2	44 ± 4	51 ± 4	54 ± 3	57 ± 4
Arterial plasma glucagon (pg/ml)							
E-SAL	42 ± 4	—	32 ± 5	31 ± 6	33 ± 9	30 ± 4	31 ± 2
E-AIC	38 ± 1	—	36 ± 5	35 ± 3	36 ± 4	32 ± 4	25 ± 1
H-SAL	29 ± 1	—	40 ± 3	41 ± 3	27 ± 4	22 ± 2	25 ± 3
H-AIC	30 ± 3	—	41 ± 4	36 ± 2	27 ± 7	28 ± 7	25 ± 5
Arterial plasma cortisol (μg/dl)							
E-SAL	1.5 ± 0.2	1.4 ± 0.3	1.8 ± 0.3	1.8 ± 0.3	2.2 ± 0.4	1.7 ± 0.3	2.5 ± 0.4
E-AIC	3.5 ± 1.0	3.3 ± 1.3	3.5 ± 1.0	2.8 ± 0.8	2.6 ± 0.5	2.6 ± 0.4	4.1 ± 1.2
H-SAL	3.2 ± 0.6	2.7 ± 1.1	4.4 ± 1.1	11.7 ± 1.7	15.1 ± 1.8	16.1 ± 2.2*	13.2 ± 2.2*
H-AIC	2.4 ± 0.3	2.0 ± 0.3	2.3 ± 0.1	9.5 ± 2.1	12.0 ± 1.7	10.1 ± 1.5*†	7.6 ± 1.5†
Arterial plasma epinephrine (pg/ml)							
E-SAL	133 ± 21	—	119 ± 28	78 ± 15	124 ± 29	100 ± 26	101 ± 17
E-AIC	181 ± 26	—	184 ± 58	138 ± 42	106 ± 26	140 ± 28	157 ± 24
H-SAL	195 ± 66	—	244 ± 154	1,172 ± 390*	1,653 ± 265*	1,312 ± 400*	899 ± 239*
H-AIC	147 ± 28	—	75 ± 24	1,517 ± 556*	1,320 ± 368*	1,418 ± 305*	1,461 ± 192*
Arterial plasma norepinephrine (pg/ml)							
E-SAL	242 ± 27	—	168 ± 26	167 ± 20	187 ± 40	197 ± 20	179 ± 46
E-AIC	196 ± 26	—	194 ± 33	171 ± 28	175 ± 49	194 ± 25	201 ± 26
H-SAL	234 ± 31	—	273 ± 81	427 ± 72*	450 ± 109*	416 ± 90*	331 ± 52
H-AIC	162 ± 30	—	117 ± 29	365 ± 100*	282 ± 69	345 ± 76	397 ± 56*

Data are means ± SE. Hyperinsulinemia was present from 0 to 150 min; intraportal AICAR was added at 60−150 min. *$P < 0.05$ vs. respective euglycemic group; †$P < 0.05$ vs. H-SAL group.

phorylation were compared using one-tailed t tests. Statistics are reported in tables and figures. Data are presented as means ± SE, and statistical significance was defined as $P < 0.05$.

RESULTS

Arterial plasma glucose, glucose infusion rates, and arterial and portal venous plasma insulin. Arterial plasma glucose levels were similar during the basal period in all groups and were clamped at euglycemic levels (104 ± 1 and 107 ± 1 mg/dl in the E-SAL and E-AIC groups, respectively) or allowed to fall to similar hypoglycemic levels (49 ± 2 and 51 ± 2 mg/dl in the H-SAL and H-AIC groups, respectively) (Fig. 2). AICAR infusion caused arterial plasma glucose to rise to 61 ± 5 mg/dl by $t = 150$ min in the H-AIC group. This increase in glucose was simulated in the H-SAL animals to 62 ± 1 mg/dl by $t = 150$ min. The mean glucose infusion rate required to simulate this rise in H-SAL animals was 1.6 ± 0.1 mg · kg^{-1} · min^{-1} (Fig. 3*B*). The glucose infusion rates required to clamp glucose at euglycemic levels during the last 90 min were similar in the presence and absence of AICAR (11.6 ± 0.4 and 11.5 ± 0.4 mg · kg^{-1} · min^{-1} in the E-SAL and E-AIC groups, respectively) (Fig. 3*A*). Arterial and portal venous plasma insulin levels were similar during the basal period in all groups and rose similarly with clamps in all groups (Table 1, Fig. 2*B*).

Arterial plasma glucagon, cortisol, and catecholamines. Arterial plasma glucagon was constant throughout the experiments at concentrations that were similar among groups (Table 1). Basal arterial plasma cortisol, epinephrine, and norepinephrine were similar in all groups. Epinephrine and norepinephrine levels rose similarly in hypoglycemic groups so that they were greater than in the euglycemic groups ($P < 0.05$). Cortisol was higher in the hypoglycemic compared with the euglycemic groups. Cortisol was greater in the H-SAL than in the H-AIC groups ($P < 0.05$) at $t = 120$ and 150 min.

Glucose kinetics. NHGO was similar during the basal period among groups and fell similarly during the first 60 min of hyperinsulinemia in each group (Fig. 4). NHGO remained suppressed in the E-SAL and H-SAL groups but was significantly increased in the E-AIC (from −0.3 ± 0.2 at $t = 60$ min to 1.4 ± 0.4 mg · kg^{-1} · min^{-1} at $t = 150$ min) and H-AIC (from 1.6 ± 0.5 at t = 60 min to 3.4 ± 0.3 mg · kg^{-1} · min^{-1} at $t = 150$ min) groups.

Endogenous R_a was similar during the basal period and fell similarly during the first 60 min of hyperinsulinemia in each group (Fig. 5). R_a remained suppressed in the E-SAL and H-SAL groups but was significantly increased in the E-AIC (from 2.2 ± 0.3 at $t = 60$ min to 4.6 ± 1.0 mg · kg^{-1} · min^{-1} at $t = 150$ min) and H-AIC (from 1.9 ± 0.5 at $t = 60$ min to 5.2 ± 0.5 mg · kg^{-1} · min^{-1} at $t = 150$ min) groups. R_d was similar during the basal period among groups and rose similarly during the first 60 min of hyperinsulinemia in the euglycemic (Fig. 6*A*) and hypoglycemic (Fig. 6*B*) groups. R_d continued to rise in the E-SAL and E-AIC groups but was significantly greater in the E-AIC compared with the E-SAL animals at $t = 120$–140 min. R_d fell in the H-SAL animals after $t = 60$ min. R_d

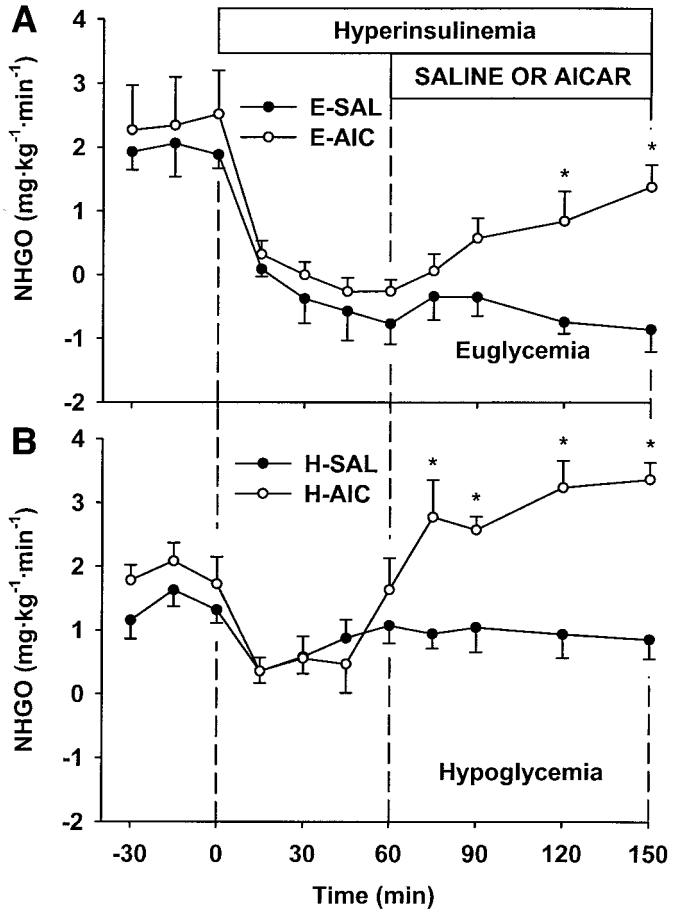

FIG. 4. Net hepatic glucose output in the saline (●) and AICAR (○) groups during the basal period (−30 to 0 min) and hyperinsulinemic-euglycemic (*A*) or -hypoglycemic (*B*) clamp period (0−150 min) in the presence or absence of intraportal AICAR from 60 to 150 min. Data are means ± SE. *Significantly different than the H-AIC group ($P < 0.05$).

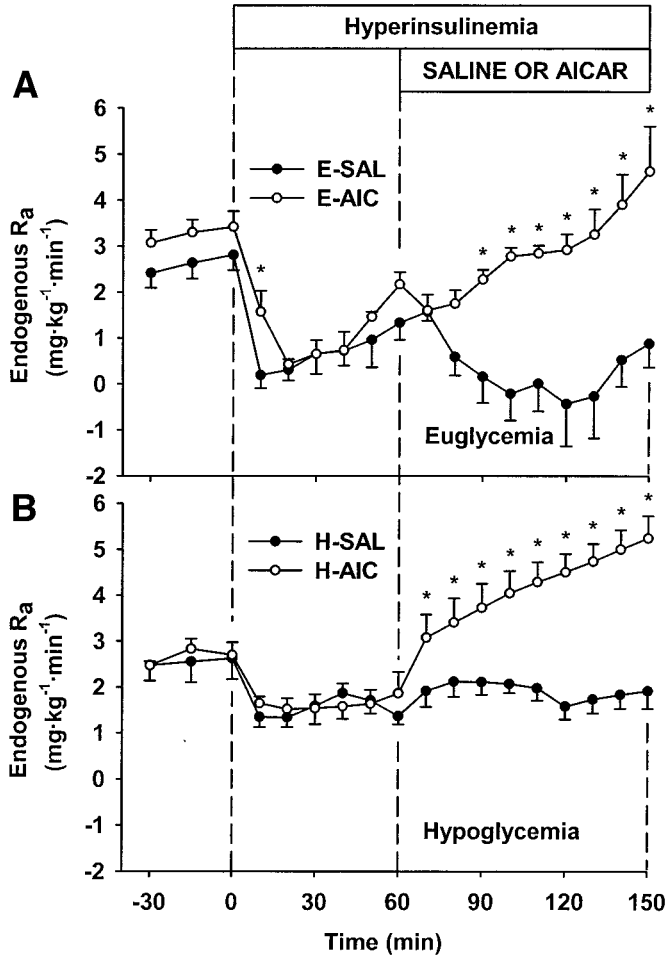

FIG. 5. Endogenous R_a rate in the saline (●) and AICAR (○) groups during the basal period (−30 to 0 min) and hyperinsulinemic-euglycemic (*A*) or -hypoglycemic (*B*) clamp period (0−150 min) in the presence or absence of intraportal AICAR from 60 to 150 min. Data are means ± SE. *Significantly different than the saline group ($P < 0.05$).

initially fell in the H-AIC group after $t = 60$ min but then rose and was significantly greater than in the H-SAL group for the final 30 min. Metabolic clearance rates showed similar results (data not shown).

Arterial concentrations and net hepatic balances of alanine, β-hydroxybutyrate, free fatty acids, glycerol, and lactate. Arterial concentrations and net hepatic balances of alanine, β-hydroxybutyrate (data not shown), free fatty acids, glycerol, and lactate were similar between the E-SAL and E-AIC animals and the H-SAL and H-AIC animals, respectively, during the basal period and first 60 min of hyperinsulinemia (Table 2). Arterial free fatty acid levels were significantly greater in the H-SAL versus the H-AIC animals at $t = 120$ min. Arterial lactate was significantly greater in the H-AIC versus the H-SAL animals from $t = 90$ min onward, as the liver had switched from a net uptake to a net output mode.

Tissue analyses. Liver glycogen and purine nucleotides are shown in Table 3. Liver glycogen was significantly decreased in the H-AIC versus the H-SAL group ($P < 0.05$). The difference in liver glycogen due to AICAR was significantly greater in the presence of hypoglycemia versus euglycemia (Fig. 7). Liver ZMP was significantly greater in AICAR- versus saline-treated groups in the presence of euglycemia or hypoglycemia ($P < 0.05$). Phosphorylation of hepatic AMPK (Thr^{172}) was similar in all groups (data not shown). Phosphorylation of hepatic ACC (Ser^{79}) was significantly greater in AICAR- versus saline-treated groups ($P < 0.05$) (Fig. 8).

Circulating liver enzymes. Circulating liver enzymes (alanine aminotransferase, aspartate aminotransferase, γ-glutamyl transpeptidase, and lactate dehydrogenase) were measured in a subset of AICAR-treated dogs. All were within normal ranges, as were circulating levels of albumin and bilirubin.

DISCUSSION

The present studies demonstrated that an intraportal infusion of AICAR at a rate of 1 mg · kg^{-1} · min^{-1} can stimulate hepatic glucose output in the presence of insulin levels that are high enough to suppress the actions of maximally effective glucagon (28). The increase in glucose output was due to a stimulation of net hepatic glycogenolysis. Moreover, these studies showed that intraportal AICAR's potent stimulation of hepatic glycogenolysis is increased under hypoglycemic conditions. In the presence of an intraportal insulin infusion of 2 mU · kg^{-1} · min^{-1}, basal intraportal glucagon replacement, and euglycemia (~100 mg/dl), intraportal AICAR increased R_a by 2.5 ± 1.0 mg · kg^{-1} · min^{-1} (Fig. 5) and decreased hepatic glycogen

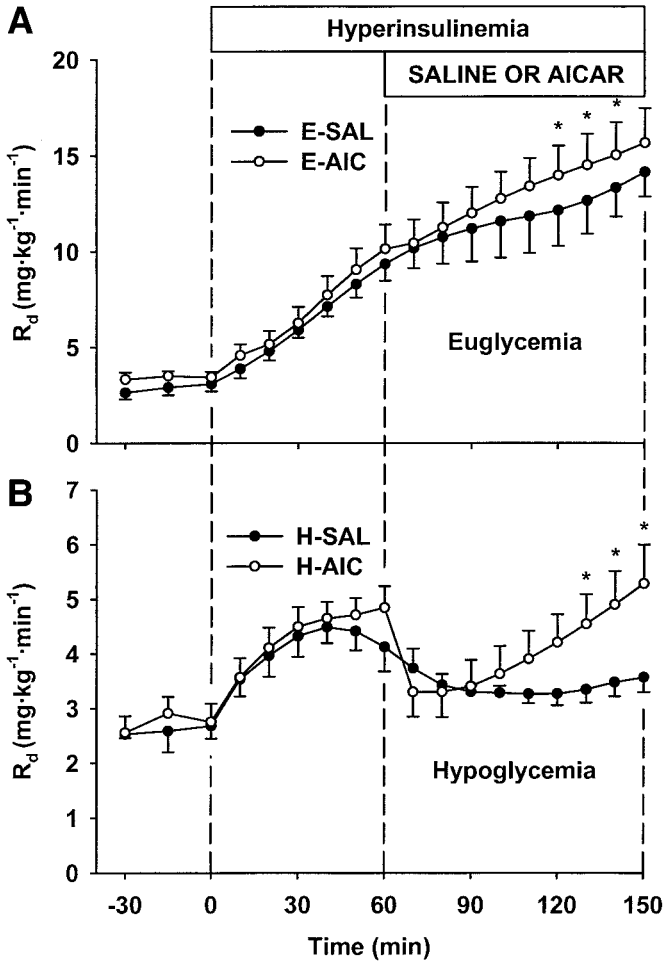

FIG. 6. Glucose utilization (R_d) rate in the saline (●) and AICAR (○) groups during the basal period (−30 to 0 min) and hyperinsulinemic-euglycemic (*A*) or -hypoglycemic (*B*) clamp period (0−150 min) in the presence or absence of intraportal AICAR from 60 to 150 min. Data are means ± SE. *Significantly different than the saline group ($P < 0.05$).

by 5 ± 3 mg/g tissue^{-1} (Fig. 7). Under hypoglycemic (~50 mg/dl) conditions, AICAR increased R_a by 3.4 ± 0.4 mg · kg^{-1} · min^{-1} and decreased hepatic glycogen by 19 ± 5 mg/g tissue^{-1}. NHGO responses paralleled increases in R_a.

Few studies have examined the hepatic effects of administering AICAR in vivo. Two recent studies have shown that intracerebroventricular infusion of AICAR increases endogenous R_a in mice (29) and rats (30). Two other studies by Bergeron and colleagues (18,19) have shown that primed (100 mg/kg) systemic AICAR doses of 7.5 (18) and 10 (19) mg · kg^{-1} · min^{-1} suppress glucose production in overnight-fasted rats. These findings were supported by the fact that injecting mice with adenoviruses expressing dominant negative AMPK (31) or treating hepatocytes with AICAR (32) increases and reduces, respectively, the expression of the key gluconeogenic enzyme, PEPCK. Moreover, AICAR has been shown to inhibit gluconeogenesis in rat hepatocytes (33). Because laboratory rats consume 80% of their total daily amount of food during nocturnal periods (34), these animals were effectively fasted for closer to 24 h, leading to a large reduction in glycogen stores in the rat. The disparities between the studies of Bergeron and colleagues and the current study showing an AICAR stimulation of glucose production can be attributed to differences in glycogen, as the liver of the 18-h−fasted dog model used in this study contained ~65 mg glycogen/g liver (35) and gluconeogenesis is only 5–25% of NHGO (36). They are unlikely to be due to a species difference, as others have reported a dramatic increase in hepatic glycogen breakdown after administration of AICAR in 5-h−fasted rats (12). Consistent with the idea that variations in hepatic glycogen levels were responsible for differences between this study and others is the fact that the marked stimulation of NHGO from a 2 mg · kg^{-1} · min^{-1} intraportal AICAR infusion was lost when given to a 42-h−fasted dog in which liver glycogen was markedly reduced (R.R.P., R.C.C., D.H.W., unpublished observation). Further support of a glycogenolytic, and not a gluconeogenic, effect is evidenced by the lack of differences in hepatic uptake of the gluconeogenic precursors, alanine and glycerol, in the presence of AICAR. Finally, supplying glucose via glycogenolysis instead of through gluconeogenesis would limit hepatic ATP usage. To assess whether AICAR infusion at the dosages used in these experiments caused liver toxicity, circulating levels of liver enzymes were measured in a subgroup of dogs. All were within predicted ranges, suggesting that liver function was normal.

The intraportal infusion of AICAR was associated with a 5 ± 3 and 19 ± 5 mg/g tissue decrease ($P < 0.05$) in hepatic glycogen in the presence of euglycemia and hypoglycemia, respectively (Table 3). Thus, hypoglycemia amplified the net hepatic glycogenolytic response to AICAR by approximately fourfold. These differences in glycogen correspond to rates of net hepatic glycogenolysis of 1.9 and 4.5 mg · kg^{-1} · min^{-1}. NHGO was 2.2 ± 0.4 mg · kg^{-1} · min^{-1} higher in the E-AIC compared with the E-SAL animals, an observation that is in line with the observed difference in net hepatic glycogenolysis (i.e., 1.9 mg · kg^{-1} · min^{-1}). NHGO was 2.5 ± 0.3 mg · kg^{-1} · min^{-1} higher in the H-AIC compared with the H-SAL group, and net hepatic lactate output was ~1.0 mg · kg^{-1} · min^{-1} greater in the H-AIC group. Together, these account for ~80% of the net hepatic glycogenolysis under hypoglycemic conditions (i.e., 4.5 mg · kg^{-1} · min^{-1}); the remaining 20% may be distributed among various other metabolic intermediates. Net hepatic lactate output was stimulated in the E-AIC group as well, although differences failed to reach significance. Stimulation of net hepatic lactate output is consistent with AMPK phosphorylation of phosphofructokinase and stimulation of glycolysis (11,37–40).

A glycogenolytic effect of AMPK is consistent with several lines of evidence. Glycogen synthase, a substrate that AMPK phosphorylates and inactivates (41), and glycogen phosphorylase, a substrate that AMPK phosphorylates and activates (15), co-immunoprecipitate with AMPK (42). A glycogen-binding domain exists on the AMPK-δ3 subunit in rat liver (43) as well as on the AMPK-β domain (43,44). A mutation in the δ3 subunit results in glycogen storage disease, at least in skeletal (45) and cardiac (46) muscle. When one considers these properties of AMPK and couples them with the effect of purine nucleotides as allosteric activators of glycogen phosphorylase (14,15, 47,48), it becomes clear that there are cellular bases for the potent effect of AICAR on hepatic glucose output.

An interesting finding of this study was that AICAR

TABLE 2
Arterial levels and net hepatic uptake of free fatty acids, glycerol, and lactate during baseline and hyperinsulinemic-euglycemic and -hypoglycemic clamp periods in the presence or absence of intraportal AICAR

		Hyperinsulinemia					
					±Intraportal AICAR		
	Basal	15 min	30 min	60 min	90 min	120 min	150 min
Arterial free fatty acids (μmol/l)							
E-SAL	485 ± 58	—	117 ± 32	79 ± 23	59 ± 17	37 ± 12	22 ± 8
E-AIC	611 ± 74	—	179 ± 55	132 ± 60	135 ± 70	124 ± 60	65 ± 41
H-SAL	643 ± 38	—	219 ± 65	979 ± 51	1,001 ± 142	862 ± 111	531 ± 64
H-AIC	745 ± 66	—	188 ± 41	903 ± 265	733 ± 244	290 ± 142*	211 ± 74
Net hepatic free fatty acid uptake (μmol · kg^{-1} · min^{-1})							
E-SAL	3.0 ± 0.4	—	0.8 ± 0.3	0.3 ± 0.1	0.2 ± 0.1	0.3 ± 0.1	0.1 ± 0.1
E-AIC	3.2 ± 0.4	—	0.5 ± 0.3	0.7 ± 0.4	0.4 ± 0.4	−0.2 ± 0.2	-0.3 ± 0.4
H-SAL	4.8 ± 0.8	—	1.4 ± 0.7	7.6 ± 2.6	5.3 ± 0.7	5.5 ± 0.5	3.3 ± 1.2
H-AIC	4.1 ± 0.4	—	1.0 ± 0.4	3.1 ± 1.3*	3.9 ± 1.8	2.2 ± 1.4*	1.0 ± 0.3
Arterial glycerol (μmol/l)							
E-SAL	48 ± 7	26 ± 7	20 ± 7	27 ± 8	18 ± 6	21 ± 8	19 ± 8
E-AIC	50 ± 5	34 ± 7	26 ± 5	23 ± 5	18 ± 4	19 ± 3	18 ± 3
H-SAL	68 ± 7	46 ± 9	39 ± 7	113 ± 13	156 ± 30	131 ± 29	143 ± 23
H-AIC	70 ± 6	43 ± 5	36 ± 2	143 ± 35	154 ± 25	132 ± 30	131 ± 33
Net hepatic glycerol uptake (μmol · kg^{-1} · min^{-1})							
E-SAL	0.7 ± 0.1	0.2 ± 0.1	0.1 ± 0.1	0.1 ± 0.1	0.1 ± 0.1	0.2 ± 0.1	0.1 ± 0.1
E-AIC	0.9 ± 0.1	0.5 ± 0.1	0.4 ± 0.1	0.3 ± 0.2	0.1 ± 0.1	0.2 ± 0.1	0.2 ± 0.1
H-SAL	1.1 ± 0.1	0.7 ± 0.1	0.5 ± 0.2	2.5 ± 0.3	3.7 ± 0.6	3.1 ± 0.6	3.4 ± 0.5
H-AIC	1.2 ± 0.1	0.6 ± 0.1	0.3 ± 0.1	2.9 ± 1.1	3.4 ± 0.8	2.2 ± 0.8	2.7 ± 0.6
Arterial lactate (μmol/l)							
E-SAL	792 ± 117	671 ± 182	765 ± 192	684 ± 120	490 ± 61	498 ± 65	585 ± 107
E-AIC	734 ± 104	569 ± 175	564 ± 132	538 ± 124	627 ± 113	663 ± 135	720 ± 161
H-SAL	569 ± 63	492 ± 76	485 ± 32	298 ± 47	617 ± 124	699 ± 194	709 ± 193
H-AIC	475 ± 102	408 ± 139	437 ± 102	546 ± 167	2,054 ± 579*	2,468 ± 904*	2,629 ± 996*
Net hepatic lactate uptake (μmol · kg^{-1} · min^{-1})							
E-SAL	−9.2 ± 1.2	−11.1 ± 3.1	−8.1 ± 1.6	−7.7 ± 2.0	−3.9 ± 1.9	−2.5 ± 2.3	−0.4 ± 2.1
E-AIC	−11.2 ± 3.2	−6.9 ± 3.0	−9.6 ± 2.2	−8.6 ± 2.6	−8.9 ± 2.8	−6.8 ± 2.7	−7.0 ± 2.9
H-SAL	−3.9 ± 2.6	−3.2 ± 3.5	−4.6 ± 3.1	4.6 ± 0.9	9.0 ± 2.4	6.6 ± 3.1	7.9 ± 2.2
H-AIC	−1.7 ± 1.7	−1.6 ± 1.6	−3.4 ± 1.0	6.0 ± 3.4	−1.8 ± 3.2*	−15.6 ± 8.7*	−7.0 ± 4.6*

Data are means ± SE. Hyperinsulinemia was present from 0 to 150 min; intraportal AICAR was added at 60−150 min. A negative number represents a net output. *$P < 0.05$ vs. H-SAL group.

reduced cortisol levels in response to hypoglycemia. AICAR was shown to have no effect on the counterregulatory hormone responses of glucagon and epinephrine to hypoglycemia when administered centrally (30), but cortisol was not measured. Our finding is consistent with the work of Fabian et al. (49), who showed that cortisol was reduced with AICAR administration to pigs after lipopolysaccharide-evoked pulmonary dysfunction after resuscitation from traumatic shock. It has been suggested that this reduction in cortisol plays a part in improving hemodynamic parameters to aid in response to stress. AICAR effects in changing cortisol (and by inference, adrenocorticotropic hormone) are consistent with this compound mediating central effects, as has been shown by other investigators (29,30,50).

In the presence of both euglycemia and hypoglycemia, intraportal AICAR significantly increased R_d (Fig. 6). This finding is consistent with those of previous studies showing that AICAR increases muscle glucose uptake (12,18–20,41,51,52). However, it is important to note that this peripheral stimulation of glucose uptake by AICAR occurred even though the dosage used in the present studies

TABLE 3
Liver glycogen and purine nucleotides after hyperinsulinemic-euglycemic and -hypoglycemic clamp periods in the presence or absence of intraportal AICAR

	E-SAL	E-AIC	H-SAL	H-AIC
Glycogen (mg/g liver)	47 ± 4	42 ± 3	52 ± 7	33 ± 5*
ZMP (μmol/g liver)	0.02 ± 0.00	2.82 ± 0.81*	0.02 ± 0.00	3.03 ± 0.45*
AMP (μmol/g liver)	0.69 ± 0.09	0.60 ± 0.12	0.33 ± 0.11	0.35 ± 0.10
ADP (μmol/g liver)	0.76 ± 0.08	0.74 ± 0.14	1.25 ± 0.29	0.57 ± 0.06
ATP (μmol/g liver)	1.06 ± 0.24	1.13 ± 0.08	1.30 ± 0.15	1.09 ± 0.08

Data are means ± SE. Nucleotide analyses: $n = 5$ in saline groups, $n = 6$ in AICAR groups. *$P < 0.05$ vs. respective saline-treated group.

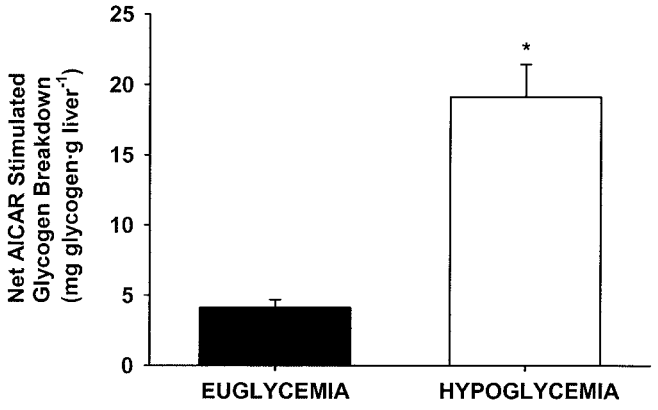

FIG. 7. Net AICAR-stimulated glycogen breakdown (calculated as Gly(H-SAL) − Gly[H-AIC] and Gly[E-SAL] − Gly[E-AIC], where Gly[H-SAL] and Gly[E-SAL] are the average hepatic glycogen levels in the respective groups, and Gly[H-AIC] and Gly[E-AIC] are the individual hepatic glycogen levels in AICAR treated dogs) after a hyperinsulinemic-euglycemic (■) or -hypoglycemic (□) clamp. Data are means ± SE. *Significantly different than the euglycemic group ($P < 0.05$).

was considerably less than that in other studies and was administered in the portal vein.

Studies have shown that one way in which AMPK is activated is by phosphorylation of the Thr^{172} residue by an upstream kinase, AMPKK or LKB1 (53–55). However, another recent study has shown that AICAR does not activate AMPK by stimulating LKB1 (56). Given that AMPK activity is regulated by both allosteric interactions as well as phosphorylation (57), phosphorylation of ACC is a more sensitive marker of AMPK activity in vivo (58). Although there was no apparent increase in the phosphorylation of the Thr^{172} residue of AMPK, the downstream target of AMPK, ACC (Ser^{79}), showed a significant increase in phosphorylation in the presence of both euglycemia and hypoglycemia (Fig. 7), proof that AMPK activity was increased. This notion is supported by work in myocardial tissue in which AICAR treatment resulted in a clear increase in the phosphorylation of ACC (14). The lower dosage of AICAR infusion used in this study may not have been high enough to cause covalent (phosphorylation) modification of AMPK, yet may have been sufficient to cause allosteric activation (14). As expected, intraportal AICAR infusion significantly increased hepatic ZMP concentrations (Table 3). Both increased AMPK activity (11,13) and increased AMP/ZMP concentrations (14,15, 17,47) have been shown to result in activation of glycogen phosphorylase. Thus, it is highly probable that the increases in net hepatic glycogen breakdown were due to increased hepatic AMPK activity and ZMP concentrations.

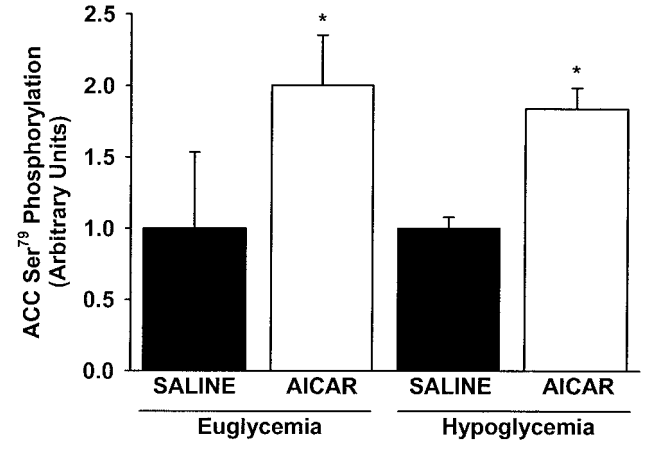

FIG. 8. Quantification of the phosphorylated form of ACC (Ser^{79}) from livers of saline-treated (■) and AICAR-treated (□) dogs after a hyperinsulinemic-euglycemic or -hypoglycemic clamp. Data are means ± SE. *Significantly different than the respective saline-treated group ($P < 0.05$).

In summary, our results show that in the presence of basal glucagon and high physiological levels of insulin, increasing hepatic ZMP levels via an intraportal infusion of AICAR stimulates endogenous glucose output via an increase in hepatic glycogenolysis and increases R_d during euglycemic and hypoglycemic conditions. Hypoglycemia amplifies the net hepatic glycogenolytic response to AICAR by approximately fourfold. These effects on hepatic and peripheral glucose metabolism occurred using infusion rates that were 10% of those previously used in rats (18–20). These responses are consistent with the concept that increased AMP concentrations not only signal increased glucose metabolism within the muscle, but also coordinate a whole-body response that increases the availability of blood glucose by stimulating glucose output by the liver. However, effects on processes such as renal glucose production, adipocyte glucose uptake, and gut glucose absorption may play a role as well. The present results combined with the results of an earlier study (17) have three important implications. First, because purine nucleotides are a natural constituent of all cells, including hepatocytes, they may comprise part of an endogenous pathway involved in the physiological activation of hepatic glucose output. Second, understanding hepatic insulin resistance caused by AICAR may provide insight into basic mechanisms underlying this liver pathology. Third, mechanisms that increase hepatic purine nucleotide concentrations may be effective in countering insulin-induced hypoglycemia. Because hypoglycemia increases AICAR-stimulated net hepatic glycogenolysis and the liver of the AICAR-infused dog appears to be relatively blind to insulin adds further weight to this third point. This suggests that a compound with similar hepatic actions could effectively be exploited to combat insulin-induced hypoglycemia, which is the single most frequently occurring complication in diabetes.

ACKNOWLEDGMENTS

This work was funded by National Institute of Diabetes and Digestive and Kidney Diseases Grant RO1-DK-50277 and Diabetes Research and Training Center Grant DK-20593.

We thank the Hormone Assay and Animal Resources Cores of the Vanderbilt Diabetes Research and Training Center for providing the hormone and catecholamine data provided.

REFERENCES

1. DCCT Research Group: The effect of intensive treatment of diabetes on the development and progression of long-term complications in insulin-dependent diabetes mellitus: the Diabetes Control and Complications Trial. *N Engl J Med* 329:977–986, 1993
2. Cryer PE: Hypoglycaemia: the limiting factor in the glycaemic management of type I and type II diabetes. *Diabetologia* 45:937–948, 2002
3. Wasserman DH, Zinman B: American Diabetes Association Technical

Review on exercise in individuals with insulin-dependent diabetes mellitus. *Diabetes Care* 17:924–937, 1994
4. Winder WW, Hardie DG: AMP-activated protein kinase, a metabolic master switch: possible roles in type 2 diabetes. *Am J Physiol* 277:E1−E10, 1999
5. Carlson CI, Winder WW: Liver AMPK-activated protein kinase and acetyl-CoA carboxylase during and after exercise. *J Appl Physiol* 86:669–674, 1999
6. Park H, Kaushik VK, Constant S, Prentki M, Przybytkowski E, Ruderman NB, Saha AK: Coordinate regulation of malonyl-CoA decarboxylase, sn-glycerol-3-phosphate acyltransferase, and acetyl-CoA carboxylase by AMP-activated protein kinase in rat tissues in response to exercise. *J Biol Chem* 277:32571–32577, 2002
7. Chen ZP, McConell GK, Michell BJ, Snow RJ, Canny BJ, Kemp BE: AMPK signaling in contracting human skeletal muscle: acetyl-CoA carboxylase and NO synthase phosphorylation. *Am J Physiol* 279:E1202−E1206, 2000
8. Fujii N, Hayashi T, Hirshman MF, Smith JT, Habinowski SA, Kaijser L, Mu J, Ljungqvist O, Birnbaum MJ, Witters LA, Thorell A, Goodyear LJ: Exercise induces isoform-specific increase in 5′AMP-activated protein kinase activity in human skeletal muscle. *Biochem Biophys Res Commun* 273:1150–1155, 2000
9. Wojtaszewski JF, MacDonald C, Nielsen JN, Hellsten Y, Hardie DG, Kemp BE, Kiens B, Richter EA: Regulation of 5′AMP-activated protein kinase activity and substrate utilization in exercising human skeletal muscle. *Am J Physiol* 284:E813−E822, 2003
10. Sabina RL, Patterson D, Holmes EW: 5-Amino-4-imidazolecarboxamide riboside (Z-riboside) metabolism in eukaryotic cells. *J Biol Chem* 260: 6107–6114, 1985
11. Young ME, Radda GK, Leighton B: Activation of glycogen phosphorylase and glycogenolysis in rat skeletal muscle by AICAR: an activator of AMP-activated protein kinase. *FEBS Lett* 382:43–47, 1996
12. Iglesias MA, Ye JM, Frangioudakis G, Saha AK, Tomas E, Ruderman NB, Cooney GJ, Kraegen EW: AICAR administration causes an apparent enhancement of muscle and liver insulin action in insulin-resistant high-fat−fed rats. *Diabetes* 51:2886–2894, 2002
13. Carling D, Hardie DG: The substrate and sequence specificity of the AMP-activated protein kinase: phosphorylation of glycogen synthase and phosphorylase kinase. *Biochim Biophys Acta* 1012:81–86, 1989
14. Longnus SL, Wambolt RB, Parsons HL, Brownsey RW, Allard MF: 5-Aminoimidazole-4-carboxamide 1-beta-D-ribofuranoside (AICAR) stimulates myocardial glycogenolysis by allosteric mechanisms. *Am J Physiol* 284: R936−R944, 2003
15. Shang J, Lehrman MA: Activation of glycogen phosphorylase with 5-aminoimidazole-4-carboxamide riboside (AICAR): assessment of glycogen as a precursor of mannosyl residues in glycoconjugates. *J Biol Chem* 279: 12076–12080, 2004
16. Aiston S, Green A, Mukhtar M, Agius L: Glucose 6-phosphate causes translocation of phosphorylase in hepatocytes and inactivates the enzyme synergistically with glucose. *Biochem J* 377:195–204, 2004
17. Pencek RR, Shearer J, Camacho RC, James FD, Lacy DB, Fueger PT, Donahue EP, Snead W, Wasserman DH: 5-aminoimidazole-4-carboxamide-1-β-D-ribofuranoside causes acute hepatic insulin resistance in vivo. *Diabetes* 54:355–360, 2004
18. Bergeron R, Russell RR 3rd, Young LH, Ren JM, Marcucci M, Lee A, Shulman GI: Effect of AMPK activation on muscle glucose metabolism in conscious rats. *Am J Physiol* 276:E938−E944, 1999
19. Bergeron R, Previs SF, Cline GW, Perret P, Russell RR 3rd, Young LH, Shulman GI: Effect of 5-aminoimidazole-4-carboxamide-1-β-D-ribofuranoside infusion on in vivo glucose and lipid metabolism in lean and obese Zucker rats. *Diabetes* 50:1076–1082, 2001
20. Shearer J, Fueger PT, Vorndick B, Bracy DP, Rottman JN, Clanton JA, Wasserman DH: AMP kinase–induced skeletal muscle glucose but not long-chain fatty acid uptake is dependent on nitric oxide. *Diabetes* 53:1429–1435, 2004
21. Leevy CM, Mendenhall CL, Lesko W, Howard MM: Estimation of hepatic blood flow with indocyanine green. *J Clin Invest* 41:1169–1179, 1962
22. Camacho RC, Pencek RR, Lacy DB, James FD, Wasserman DH: Suppression of endogenous glucose production by mild hyperinsulinemia during exercise is determined predominantly by portal venous insulin. *Diabetes* 53:285–293, 2004
23. Lloyd B, Burrin J, Smythe P, Alberti KG: Enzymatic fluorometric continuous-flow assays for blood glucose, lactate, pyruvate, alanine, glycerol, and 3-hydroxybutyrate. *Clin Chem* 24:1724–1729, 1978
24. Chan T, Exton J: A rapid method for the determination of glycogen content and radioactivity in small quantities of tissue or isolated hepatocytes. *Anal Biochem* 71:96–105, 1976
25. Ally A, Park G: Rapid determination of creatine, phosphocreatine, purine bases and nucleotides (ATP, ADP, AMP, GTP, GDP) in heart biopsies by gradient ion-pair reversed-phase liquid chromatography. *J Chromatogr* 575:19–27, 1992
26. Wynants J, Van Belle H: Single-run high-performance liquid chromatography of nucleotides, nucleosides, and major purine bases and its application to different tissue extracts. *Anal Biochem* 144:258–266, 1985
27. Mari A: Estimation of the rate of appearance in the non-steady state with a two-compartment model. *Am J Physiol* 263:E400–E415, 1992
28. Steiner KE, Williams PE, Lacy WW, Cherrington AD: Effects of insulin on glucagon-stimulated glucose production in the conscious dog. *Metabolism* 39:1325–1333, 1990
29. Perrin C, Knauf C, Burcelin R: Intracerebroventricular infusion of glucose, insulin and the AMP-activated kinase activator AICAR controls muscle glycogen synthesis. *Endocrinology* 145:4025–4033, 2004
30. McCrimmon RJ, Fan X, Ding Y, Zhu W, Jacob RJ, Sherwin RS: Potential role for AMP-activated protein kinase in hypoglycemia sensing in the ventromedial hypothalamus. *Diabetes* 53:1953–1958, 2004
31. Yamauchi T, Kamon J, Minokoshi Y, Ito Y, Waki H, Uchida S, Yamashita S, Noda M, Kita S, Ueki K, Eto K, Akanuma Y, Froguel P, Foufelle F, Ferre P, Carling D, Kimura S, Nagai R, Kahn BB, Kadowaki T: Adiponectin stimulates glucose utilization and fatty-acid oxidation by activating AMP-activated protein kinase. *Nat Med* 8:1288–1295, 2002
32. Lochhead PA, Salt IP, Walker KS, Hardie DG, Sutherland C: 5-aminoimidazole-4-carboxamide riboside mimics the effects of insulin on the expression of the two key gluconeogenic genes PEPCK and glucose-6-phosphatase. *Diabetes* 49:896–903, 2000
33. Vincent MF, Marangos PJ, Gruber HE, Van den Berghe G: Inhibition by AICA riboside of gluconeogenesis in isolated rat hepatocytes. *Diabetes* 40:1259–1266, 1991
34. Sidlo J, Zaviacic M, Kvasnicka P: Night and day differences in the food intake of laboratory rats Wistar and Koletsky strains. *Bratisl Lek Listy* 96:655–657, 1995
35. Moore MC, Pagliassotti MJ, Wasserman DH, Goldstein R, Asher J, Neal DW, Cherrington AD: Hepatic denervation alters the transition from the fed to the food-deprived state in conscious dogs. *J Nutr* 123:1739–1746, 1993
36. Connolly CC, Steiner KE, Stevenson RW, Neal DW, Williams PE, Alberti KGMM, Cherrington AD: Regulation of glucose metabolism by norepinephrine in conscious dogs. *Am J Physiol* 261:E764–E772, 1991
37. Halse R, Fryer LG, McCormack JG, Carling D, Yeaman SJ: Regulation of glycogen synthase by glucose and glycogen: a possible role for AMP-activated protein kinase. *Diabetes* 52:9–15, 2003
38. Atkinson LL, Kozak R, Kelly SE, Onay Besikci A, Russell JC, Lopaschuk GD: Potential mechanisms and consequences of cardiac triacylglycerol accumulation in insulin-resistant rats. *Am J Physiol* 284:E923−E930, 2003
39. Hue L, Beauloye C, Marsin AS, Bertrand L, Horman S, Rider MH: Insulin and ischemia stimulate glycolysis by acting on the same targets through different and opposing signaling pathways. *J Mol Cell Cardiol* 34:1091–1097, 2002
40. Marsin AS, Bouzin C, Bertrand L, Hue L: The stimulation of glycolysis by hypoxia in activated monocytes is mediated by AMP-activated protein kinase and inducible 6-phosphofructo-2-kinase. *J Biol Chem* 277:30778–30783, 2002
41. Wojtaszewski JF, Jorgensen SB, Hellsten Y, Hardie DG, Richter EA: Glycogen-dependent effects of 5-aminoimidazole-4-carboxamide (AICA)-riboside on AMP-activated protein kinase and glycogen synthase activities in rat skeletal muscle. *Diabetes* 51:284–292, 2002
42. Chen Z, Heierhorst J, Mann RJ, Mitchelhill KI, Michell BJ, Witters LA, Lynch GS, Kemp BE, Stapleton D: Expression of the AMP-activated protein kinase β1 and β2 subunits in skeletal muscle. *FEBS Lett* 460:343–348, 1999
43. Polekhina G, Gupta A, Michell BJ, van Denderen B, Murthy S, Feil SC, Jennings IG, Campbell DJ, Witters LA, Parker MW, Kemp BE, Stapleton D: AMPK β subunit targets metabolic stress sensing to glycogen. *Curr Biol* 13:867–871, 2003
44. Hudson ER, Pan DA, James J, Lucocq JM, Hawley SA, Green KA, Baba O, Terashima T, Hardie DG: A novel domain in AMP-activated protein kinase causes glycogen storage bodies similar to those seen in hereditary cardiac arrhythmias. *Curr Biol* 13:861–866, 2003
45. Milan D, Jeon JT, Looft C, Amarger V, Robic A, Thelander M, Rogel-Gaillard C, Paul S, Iannuccelli N, Rask L, Ronne H, Lundstrom K, Reinsch N, Gellin J, Kalm E, Roy PL, Chardon P, Andersson L: A mutation in PRKAG3 associated with excess glycogen content in pig skeletal muscle. *Science* 288:1248–1251, 2000
46. Arad M, Benson DW, Perez-Atayde AR, McKenna WJ, Sparks EA, Kanter RJ, McGarry K, Seidman JG, Seidman CE: Constitutively active AMP

kinase mutations cause glycogen storage disease mimicking hypertrophic cardiomyopathy. *J Clin Invest* 109:357–362, 2002
47. Ercan-Fang N, Gannon MC, Rath VL, Treadway JL, Taylor MR, Nuttall FQ: Integrated effects of multiple modulators on human liver glycogen phosphorylase A. *Am J Physiol* 283:E29−E37, 2002
48. Newgard CB, Hwang PK, Fletterick RJ: The family of glycogen phosphorylases: structure and function. *Crit Rev Biochem Mol Biol* 24:69–99, 1989
49. Fabian TC, Fabian MJ, Yockey JM, Proctor KG: Acadesine and lipopolysaccharide-evoked pulmonary dysfunction after resuscitation from traumatic shock. *Surgery* 119:302–315, 1996
50. Minokoshi Y, Alquier T, Furukawa N, Kim YB, Lee A, Xue B, Mu J, Foufelle F, Ferre P, Birnbaum MJ, Stuck BJ, Kahn BB: AMP-kinase regulates food intake by responding to hormonal and nutrient signals in the hypothalamus. *Nature* 428:569–574, 2004
51. Merrill GF, Kurth EJ, Hardie DG, Winder WW: AICA riboside increases AMP-activated protein kinase, fatty acid oxidation, and glucose uptake in rat muscle. *Am J Physiol* 273:E1107–E1112, 1997
52. Kurth-Kraczek EJ, Hirshman MF, Goodyear LJ, Winder WW: 5′ AMP-activated protein kinase activation causes GLUT4 translocation in skeletal muscle. *Diabetes* 48:1667–1671, 1999
53. Lizcano JM, Goransson O, Toth R, Deak M, Morrice NA, Boudeau J, Hawley SA, Udd L, Makela TP, Hardie DG, Alessi DR: LKB1 is a master kinase that activates 13 kinases of the AMPK subfamily, including MARK/PAR-1. *EMBO J* 23:833–843, 2004
54. Woods A, Johnstone SR, Dickerson K, Leiper FC, Fryer LG, Neumann D, Schlattner U, Wallimann T, Carlson M, Carling D: LKB1 is the upstream kinase in the AMP-activated protein kinase cascade. *Curr Biol* 13:2004–2008, 2003
55. Hawley SA, Boudeau J, Reid JL, Mustard KJ, Udd L, Makela TP, Alessi DR, Hardie DG: Complexes between the LKB1 tumor suppressor, STRADα/β and MO25α/β are upstream kinases in the AMP-activated protein kinase cascade. *J Biol* 2:28, 2003
56. Sakamoto K, Goransson O, Hardie DG, Alessi DR: Activity of LKB1 and AMPK-related kinases in skeletal muscle: effects of contraction, phenformin, and AICAR. *Am J Physiol* 287:E310−E317, 2004
57. Corton JM, Gillespie JG, Hawley SA, Hardie DG: 5-aminoimidazole-4-carboxamide ribonucleoside: a specific method for activating AMP-activated protein kinase in intact cells? *Eur J Biochem* 229:558–565, 1995
58. Al-Khalili L, Krook A, Zierath JR, Cartee GD: Prior serum and AICAR-induced AMPK activation in primary human myocytes does not lead to subsequent increase in insulin-stimulated glucose uptake. *Am J Physiol* 287:E553−E557, 2004